NASA CONTRACTOR REPORT

NASA CR-1023

GPO PRICE $ _____

CFSTI PRICE(S) $ _____

Hard copy (HC) 3.00

Microfiche (MF) .65

ff 653 July 65

FACILITY FORM 602

(ACCESSION NUMBER) (THRU)

(PAGES) (CODE)

(NASA CR OR TMX OR AD NUMBER) (CATEGORY)

NASA CR-1023

RADIATION HEAT TRANSFER IN ABSORBING, SCATTERING, AND EMITTING MEDIUM

by F. Shahrokhi and P. Wolf

Prepared by

THE UNIVERSITY OF TENNESSEE SPACE INSTITUTE

Tullahoma, Tenn.

for

NATIONAL AERONAUTICS AND SPACE ADMINISTRATION • WASHINGTON, D. C. • APRIL 1968

NASA CR-1023

RADIATION HEAT TRANSFER IN ABSORBING, SCATTERING, AND EMITTING MEDIUM

By F. Shahrokhi and P. Wolf

Distribution of this report is provided in the interest of information exchange. Responsibility for the contents resides in the author or organization that prepared it.

Prepared under Grant No. NGR-43-001-021 by
THE UNIVERSITY OF TENNESSEE SPACE INSTITUTE
Tullahoma, Tenn.

for

NATIONAL AERONAUTICS AND SPACE ADMINISTRATION

For sale by the Clearinghouse for Federal Scientific and Technical Information
Springfield, Virginia 22151 – CFSTI price $3.00

RADIATION HEAT TRANSFER IN ABSORBING, SCATTERING, AND EMITTING MEDIUM

F. Shahrokhi* and P. Wolf+

The University of Tennessee Space Institute
Tullahoma, Tennessee

ABSTRACT

In recent times several articles have been published in which the radiative heat flow is computed between plane parallel, plates with anisotropically scattering atmosphere. An involved analytical treatment employing matrix calculus and a computer program as long and involved as the mathematical analysis was used.

Work presented herein indicates that a usable solution to the problem can be obtained by simple iteration of the set of equations which result from approximation of the equation of radiation transfer. The iteration worked perfectly, the computer program is simple and short, and the method can accomodate the same, if not more, parameter variations than the more analytical treatments.

This study was carried out as part of a research program being performed under NASA Sustaining Grant NGR-43-001-021

*Assistant Professor of Aerospace Engineering

+Graduate Research Assistant

INTRODUCTION

The solution giving the radiant heat transfer between 2 parallel plates with an anisotropically scattering, absorbing and emitting gas in the space between the plates for one-dimensional conditions was presented by (1) (2). By computing monochromatic heat flow values, changes in gas- and wall-radiation- properties could be fully accounted for. The scattering mechanism was introduced by the Mie-theory (3). The scattering function may also be taken from results of measurements (4). To represent the solution, the previous authors took the equation of radiation transfer in its one-dimensional form and approximated the integral by Gauss-quadrature. This approach produces a system of equations of an order according to the order of the quadratures. The whole vector of discrete radiation intensity values was then computed by matrix methods, which with the boundary conditions at the two walls and for arbitrary gas temperatures, resulted in an extensive computer program.

Because of the quadrature approximations the results will have a definite error, particularly for gases with high temperature gradient.

The method used herein is to evaluate the system of equations resulting from the equation of transfer by direct iteration using finite difference methods. The computer calculation for the intensities converges sufficiently and can accomodate very

arbitrary and abrupt temperature gradients in the gas. This latter capability is important for radiation heat flux analysis e.g. through strongly scattering boundary layers. The program is straight-forward and the heat fluxes can be computed at any position in the gas layer.

The iteration scheme can be linked into a calculation loop for not only radiative but also conduction and convection heat transfer.

Since in boundary layer type flows the changes in one direction (y) are much higher than in the other (x, along the stream) the one-dimensional approach for the radiant heat flux will be a reasonable approximation to the two-dimensional case.

ANALYSIS

The thermal radiation intensity in a participating medium is described by the equation of transfer:

$$(\bar{s} \cdot \bar{\nabla}) I_\nu(\bar{r},\bar{s}) = -\rho\beta_\nu I_\nu(\bar{r},\bar{s}) + \frac{\rho\sigma_\nu}{4\pi}\int_{4\pi}\int S(\bar{s},\bar{s}') I_\nu(\bar{r},\bar{s}) \cdot dw' + \rho\kappa_\nu I_{bb_\nu} \qquad (1)$$

The scattering function $S(\bar{s},\bar{s}')$ is normalized, and the scattering coefficient σ_ν gives the amount of scattered radiation. $\bar{s}$, $\bar{s}'$ are unit vectors describing a direction in geometrical space. For the one-dimensional case (see Figure 1), this means the scattering properties are only x-dependent. The plates are infinitely large and of uniform temperature. Equation 1 becomes

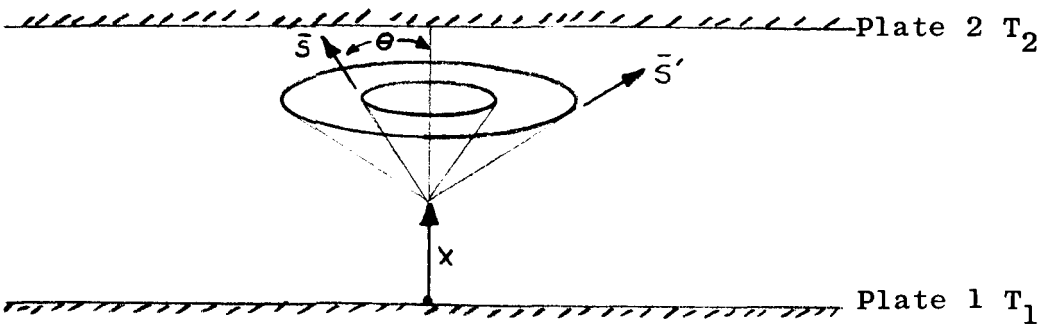

Fig. 1

$$\cos\theta \cdot \frac{dI(x,\theta)}{dx} = -\rho\beta I(x,\theta) + \frac{\rho\sigma}{4\pi}\int_{\theta'=0}^{\pi}\int_{\varphi'=0}^{2\pi} S(\bar{\alpha})\ I(x,\theta') \sin\theta'\, d\theta'\, d\varphi' + \rho\kappa\, I_{bb} \qquad (2)$$

The frequency notation has been dropped for clarity of presentation. $S(\bar{\alpha})$ is taken to be the axially symmetric scattering function, and $\bar{\alpha}$ is the angle between incoming and scattered ray.

With I being a function of position x and the angle θ only, it can be written (reference (1)):

$$S(\mu,\mu') = \frac{1}{2\pi}\int_{0}^{2\pi} S(\bar{\alpha})\, d\varphi' \qquad \cos\theta = \mu \qquad (3)$$

The integral becomes:

$$\int_{-1}^{+1} I(x,\ \mu')\Big\{\int_{0}^{2\pi} S(\alpha)\ d\varphi'\Big\}\ d\mu' = 2\pi\int_{-1}^{+1} I(x\mu')S(\mu,\mu')d\mu' \qquad (4)$$

and Equation 2:

$$\mu \frac{dI}{dx} = \rho\beta I + \frac{\rho\sigma}{2} \int_{-1}^{+1} I(x\mu')S(\mu\mu')d\mu' + \rho\kappa\, I_{bb}$$

$$\frac{dI}{dx} = -\frac{\rho\beta}{\mu} I + \frac{\rho\sigma}{2\mu} \int_{-1}^{+1} I(x\mu')S(\mu,\mu')d\mu' + \frac{\rho\kappa}{\mu}\, I_{bb} \qquad (5)$$

The streams of intensity will be treated separately, because of their independence of each other at the walls (5). I^+ is the intensity in a direction toward wall 2, I^- is the intensity in the reverse or backward direction. The integral will be approximated by Gauss quadrature, μ_i and μ_j are discrete direction cosines for the quadrature points.

$$\frac{dI_i^+}{dx} = -\frac{\rho\beta}{\mu_i} I_i^+ + \frac{\rho\sigma}{2\mu_i} \sum_{j=1}^{k} a_j (S(\mu_i\mu_j)I_j^+ + S(\mu_i-\mu_j)I_j^-) + \frac{\rho\kappa}{\mu_i} I_{bb} \qquad (6a)$$

k = order of the quadrature i = 1, 2, 3, . . . k

$$\frac{dI^-_i}{dx} = \frac{\rho\beta}{\mu_i} I^-_i - \frac{\rho\sigma}{2\mu_i} \sum_{j=1}^{k} a_j (S(-\mu_i\mu_j)I^+_j + S(-\mu_i-\mu_j)I^-_j) - \frac{\rho\kappa}{\mu_i} I_{bb} \qquad (6b)$$

(signs changed because $\mu_{-i} = -\mu_i$)

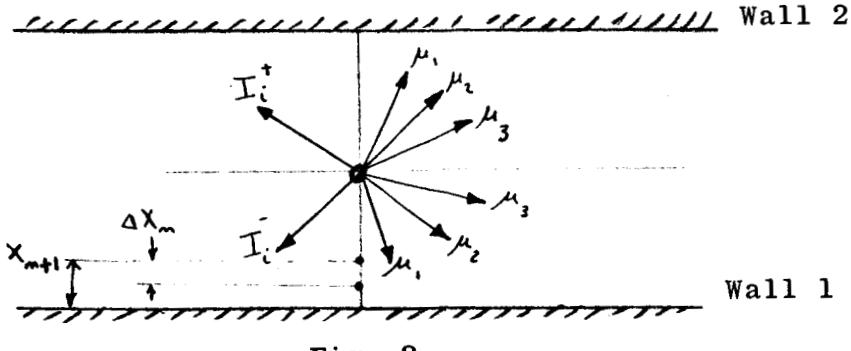

Fig. 2

A finite difference quotient may now be introduced for the differential $\frac{dI_i}{dx}$. Forward, backward or centered differences may be used.

$$\left(\frac{dI_i}{dx}\right)_{\text{at position } n} = \frac{I_{i_{n+1}} - I_{i_n}}{\Delta x} \text{ or } = \frac{I_{i_n} - I_{i_{n-1}}}{\Delta x} \text{ or } = \frac{I_{i_{n+1}} - I_{i_{n-1}}}{2 \cdot \Delta x}$$

Computations were made with the three representations. The simple forward and backward quotients resulted in a more stable iteration scheme with a 50 times higher possible step size, Δx than the centered quotient permitted. The truncation error for the simple quotients is in the order of magnitude of Δx compared to that of $(\Delta x)^2$ for the centered quotient. In spite of the larger error of the simple quotients, it was established that the accuracy of the simple quotients was consistent with possible errors introduced by the quadrature.

The results for simple quotient differed by 2% at most from those with the centered quotient at the highest comparable step size Δx.

Thus the simple representation of the derivatives was chosen finally:

$$I_{i}^{+}{}_{n+1} - I_{i}^{+}{}_{n} = -\frac{\rho\beta\Delta x}{\mu_i} I_{i}^{+}{}_{n} + \frac{\rho\sigma\Delta x}{2\mu_i} \sum_{j=1}^{k} a_j (S_{ij} I_{j}^{+}{}_{n} + S_{i-j} I_{jn}^{-}) + \frac{\rho\kappa\Delta x}{\mu_i} I_{bb_n}$$

$$I_{i}^{-}{}_{n+1} - I_{i}^{-}{}_{n} = \frac{\rho\beta\Delta x}{\mu_i} I_{i}^{-}{}_{n} \frac{\rho\sigma\Delta x}{2\mu_i} \sum_{j=1}^{k} a_j (S_{-ij} I_{j}^{+}{}_{n} + S_{-i-j} I^{-}{}_{jn}) - \frac{\rho\kappa\Delta x}{\mu_i} I_{bb_n}$$

$$I_{i_{n+1}}^{+} = \left(1 - \frac{\rho\beta\Delta x}{\mu_i}\right) I_{i_n}^{+} + \frac{\rho\sigma\Delta x}{2\mu_i} \sum_{j=1}^{k} a_j \left(S_{ij} I_{j_n}^{+} + \frac{\rho\kappa\Delta x}{\mu_i} I_{bb_n}\right) \quad (7a)$$

$$I_{i_{n+1}}^{-} = \left(1 + \frac{\rho\beta\Delta x}{\mu_i}\right) I_{i_n}^{-} - \frac{\rho\sigma\Delta x}{2\mu_i} \sum_{j=1}^{k} a_j \left(S_{-ij} I_{jn}^{+} + S_{-i-j} I_{jn}^{-}\right) - \frac{\rho\kappa\Delta x}{\mu_i} I_{bb_n} \qquad i = 1, 2, 3 \ldots k \quad (7b)$$

These equations express the intensity in a direction $+\mu_i$ or $-\mu_i$ at a position (n + 1) on the x-axis in terms of the conditions at point (n), see Figure 2.

$I_{i_{n+1}}^{+}$ and $I_{i_{n+1}}^{-}$ are vectors of k components. Equations 7 are the essential equations for the iteration on the computer.

BOUNDARY CONDITIONS

The radiation flux directed to the walls is partly absorbed and partly reflected. Additionally, the walls emit radiation. The walls will be introduced as diffusely reflecting. This condition can easily be removed as soon as the reflection properties of the walls are known.

Outgoing intensity at wall 1:

$$I(x = 0, \mu_i) = \epsilon_1 \cdot I_{bb_1} + \rho_1 \cdot 2 \sum_{j=1}^{k} a_j \mu_j I(x = 0, -\mu_j)$$

The first part is the emission of the wall, the second part is the reflected heat flux, the sum is the quadrature expression of the incoming flux:

$$\frac{F^-}{\pi} = \frac{1}{\pi} \int_{\varphi=0}^{2\pi} \int_{\theta=\pi/2}^{\pi} I(x = 0, \theta)\cos\theta \sin\theta \, d\theta \, d\varphi$$

$$= -2 \int_{0}^{-1} \mu \, I(\varphi, \mu) \, d\mu = 2 \sum_{j=1}^{k} a_j \mu_j I_j^- \quad (o)$$

$$I_{i_1}^+ = (1 - \rho_1) I_{bb_1} + 2\rho_1 \sum_{j=1}^{k} a_j \mu_j \, I_{j_1}^- \qquad (8)$$

Similarly for wall 2 with N the total number of integration steps, N lying on wall 2

$$I_{i_N}^- = (1 - \rho_2) \, I_{bb_N} + 2\rho_2 \sum_{j=1}^{k} a_j \mu_j \, I_{j_N}^+ \qquad (9)$$

$$i = 1, 2, 3. \ . \ . \ k$$

This shows that the boundary conditions depend on the solution in the field, because the incoming intensities at each wall must be known to express the outgoing intensities which represent the boundary conditions.

These outgoing intensities are equal for all directions μ_i because of the diffuse-wall-assumption.

THE ITERATION SCHEME

Because of the peculiar boundary conditions the iteration is started in three steps.

First, assuming no participating medium the outgoing intensity is computed for one wall

$$I_{i_1}^+ = \frac{\epsilon_N}{\epsilon_1 + \epsilon_N - \epsilon_1 \cdot \epsilon_N} \cdot I_{bb_1} \quad (T_1) \qquad (10a)$$

or

$$I^-_{i_N} = \frac{\epsilon_1}{\epsilon_1 + \epsilon_N - \epsilon_1 \epsilon_N} I_{bb_N}(T_N) \qquad (10b)$$

for two plane parallel plates of emissivity ϵ_1 and ϵ_N and temperatures T_1 and T_N.

One of these results is taken to start the iteration under the assumption that the gas absorbs and emits only, which reduces the equations (7) to simply

$$I^+_{i_{n+1}} = (1 - \frac{\rho\kappa\Delta x}{\mu_i}) I^+_{i_n} + \frac{\rho\kappa\Delta x}{\mu_i} I_{bb_n} \qquad (11a)$$

$$I^-_{i_{n+1}} = (1 + \frac{\rho\kappa\Delta x}{\mu_i}) I^-_{i_n} - \frac{\rho\kappa\Delta x}{\mu_i} I_{bb_n} \qquad (11b)$$

This step is necessary because the backward intensities I^-_i are not yet known, if the computation is started at wall 1 and steps forward to wall 2. The scattering sum in Equation (7) can not be computed at this stage. Note that the extinction coefficient β has to be replaced by the absorption κ here.

The iteration arrives with (11a) at wall 2, boundary condition (9) can be computed and now under use of a backward finite difference quotient

$$\frac{dI}{dx} \simeq \frac{In - In-1}{\Delta x} = \frac{In-1 - In}{-\Delta x}$$

the calculation can go back to wall 1

$$I^-_{i_{n-1}} = (1 - \frac{\rho\kappa\Delta x}{\mu_i}) I^-_{i_n} + \frac{\rho\kappa\Delta x}{\mu_i} I_{bb_n} \qquad (12)$$

Here boundary condition (8) is used to compute a better value $I^+_{i_1}$.

This iteration is run until the difference between two successive values of one particular intensity does not differ by more than 5%. For the intensity was taken the wall intensity $I^+_{i_1}$, because this insured that all other I values would be accurate enough.

The intensity field thus computed is taken as initial values for the final iteration with scattering included. Compute with (7a) to wall 2, use boundary condition (9) and use

$$I^-_{i_{n-1}} = (1 - \frac{\rho\varrho\Delta x}{\mu_i})\ I^-_{i_n} + \frac{\rho\sigma\Delta x}{2\mu_i} \sum_{j=1}^{k} a_j (S_{-ij} I^+_{j_n} + S_{-i-j} I^-_{j_n}) + \frac{\rho\kappa\Delta x}{\mu_i} I_{bb_n} \qquad (13)$$

on the way back from wall 2 to wall 1

Use boundary condition (8) to turn around at wall 1 for the next iteration step.

This iteration was stopped when the wall intensity $I^+_{i_1}$ did not deviate for more than 0.01% between two successive iterated values.

With the whole intensity field given, the monochromatic heat flux at every position n can easily be computed

$$Q_\nu(x_n) = 2\pi \int_{\mu=0}^{\pi/2} (I^+_n(\mu) - I^-_n(\mu))\ \mu\ d\mu$$

with quadrature

$$Q_{\nu_n} = 2\pi \sum_{j=1}^{k} a_j \mu_j\ (I^+_{n_j} - I^-_{n_j}) \qquad (14)$$

The black body intensity is

$$I_{bb}(T) = \frac{2h\nu^3}{c^2} \cdot \frac{1}{\exp(\frac{h\nu}{kT}) - 1} \qquad (15)$$

Equations 7a,8, 9, 10a, 11a, 12, 13, 14, 15 are the basis of the computer program. Temperature functions $T(x) \rightarrow T_1, T_2, T_3 \ldots T_n$ were created in a sub-program.

The scattering functions $S(\mu_i\mu_j) = S_{ij}$ were taken from (1) for Mie scattering.

$$S(\mu\mu') = 1 + \sum_{n=1}^{n=\infty} a_n P_n (\mu\ \mu') \qquad (16)$$

with a_n tabulated in (6), P_n tabulated in (7), σ, β, κ values were taken from (1) and (7).

The iteration needs, at the most, 5 to 10 iteration steps to arrive at the required accuracy and consumes very little computer time.

So the monochromatic heat fluxes for 15 to 20 frequencies may easily be computed; and, with a numerical integration (trapezoidal or Simpson method), the total radiant heat flux can be found:

$$Q_R = \int_o^\infty Q_{R\nu} d\nu$$

For this integration is is permissible to assume that the thermal radiation at the usual temperatures is in the frequency band:

$$10^{10} \frac{1}{\text{sec}} \leq \nu \leq 10^{15} \frac{1}{\text{sec}}$$

Since the heat flux computation is worked on 100 to 300 points on the space coordinate, a precise picture of the local

heat flux can be given from wall to wall, and also the heat-source distribution can be computed:

$$Q_S(x_n) = \frac{Q_R(x_{n+1}) - Q_R(x_n)}{\Delta x} \qquad (17)$$

Discussion of Results

To check the iteration method for errors and general accuracy, results were compared to those of (2) for one data set (see Figure 3 and Figure 4). The figures give the ratio of the wall heat fluxes at wall 1 (Figure 3) and at wall 2 (Figure 4) with scattering to the wall heat fluxes for no participating medium and black walls for a range of relative particle sizes and linear temperature distribution in the gas. The deviations between the results of the two methods are written into the figures. The maximum is +18%. The following reasons will account for the differences: Author (2) used only a third order quadrature for the intensity scattering integral, whereas the iteration was worked in fourth order quadrature, double precision, 250 steps on the x-coordinate. Comparison runs with the iteration showed that results from third order quadrature differ up to 15% from those of fourth order approximation for higher α -values where the scattering function develops very steep peaks for forward and backward scattering.

The method (2) approximates the temperature profile by a polynomial which was in the number calculations of seventh order; the iteration method uses the temperatures at as many points as there are finite difference steps, in the number calculations actually 250.

It was observed that the radiant transfer process is very sensitive to even small temperature changes. Thus it seems necessary to represent the given temperature profile as true as possible; but it cannot be said quantitatively what error is introduced by using an approximating polynomial for the temperature profile.

Comparison runs of the iteration method with forward-backward finite difference quotient and with centered finite difference quotient (truncation error proportional to the step size Δx and proportional to $(\Delta x)^2$ respectively) showed that using the simple forward-backward representation with its high iteration stability range deviates at the most for 2% from the results with centered finite difference quotient.

To make the errors due to low order quadrature approximation small, the safest means is to increase the order of quadrature. This can be done with no complications at all for the iteration method, provided the integrated Legendre polynomials are worked out for higher order quadratures.

Figures 5 to 8 show typical results of the iteration method, giving the radiant heat flux as a continuous function throughout the gas layer, and giving the corresponding heat source distribution dictated by the assumed linear temperature distribution in the gas. For the total radiant heat flux the monochromatic heat fluxes and also the heat source distributions--would have to be summed up over the frequencies.

Figures 5 to 8 show that for linear gas temperature the radiation heat flux is much higher in the center region than close to the walls. The gradients are high in the wall regions. The gas layer at the hot wall has strong heat sources to keep the highly emitting layer at the linear temperatures, whereas in the gas layer close to the cold wall there are strong heat sinks to keep the highly absorbing particles at their low linear temperatures.

If these sources and sinks did not exist, the temperature profile in the gas layer would change toward the radiation equilibrium temperature profile shape, the gas layer close to the hot wall would be much cooler, and the gas close to the cold wall would be much hotter than the linear temperature profile says.

To minimize errors due to high local gradients as they turned out for linear temperatures, the step size in the iteration method can be varied so as to decrease the size of increment Δx with high gradients.

A great number of heat flux computations has to be run in order to analyze the effects of particle sizes, particle materials, wall properties, wall temperatures, etc., on radiant transfer and to find the ways to influence it by suitable seeds or ablation layers. The immediate knowledge of the heat fluxes throughout the region is of great help. For this reason, it is thought that the iteration method presents an appreciably better means than the earlier methods.

References

1. T. J. Love, Jr., An Investigation of Radiant Heat Transfer in Absorbing, Emitting and Scattering Media; Aeronautic. Research Lab., ARL 63-3.

2. H. M. Hsia, Radiative Transfer in an Absorbing Anisotropic Scattering and Non-Isothermal Medium between Parallel Plates; Ph.D. Thesis, University of Oklahoma.

3. G. Mie, Ann. Physik 25, 1908.

4. T. J. Love, J. F. Beattie, Experimental Determination of Thermal Radiation Scattering by Small Particles; Aerospace Research Lab., ARL 65-110.

5. S. Chandrasekhar, Radiative Transfer; Dover Publications, Inc; New York.

6. C. M. Chu, G. C. Clark, S. W. Churchill, Tables of Angular Distribution Coefficients for Light Scattering Spheres; Engineering Research Inst., University of Michigan, 1957.

7. F. C. Chromey, Evaluation of Mie Equations for Colored Spheres; T. Optic. Society America, Vol. 50, No. 7, 1960.

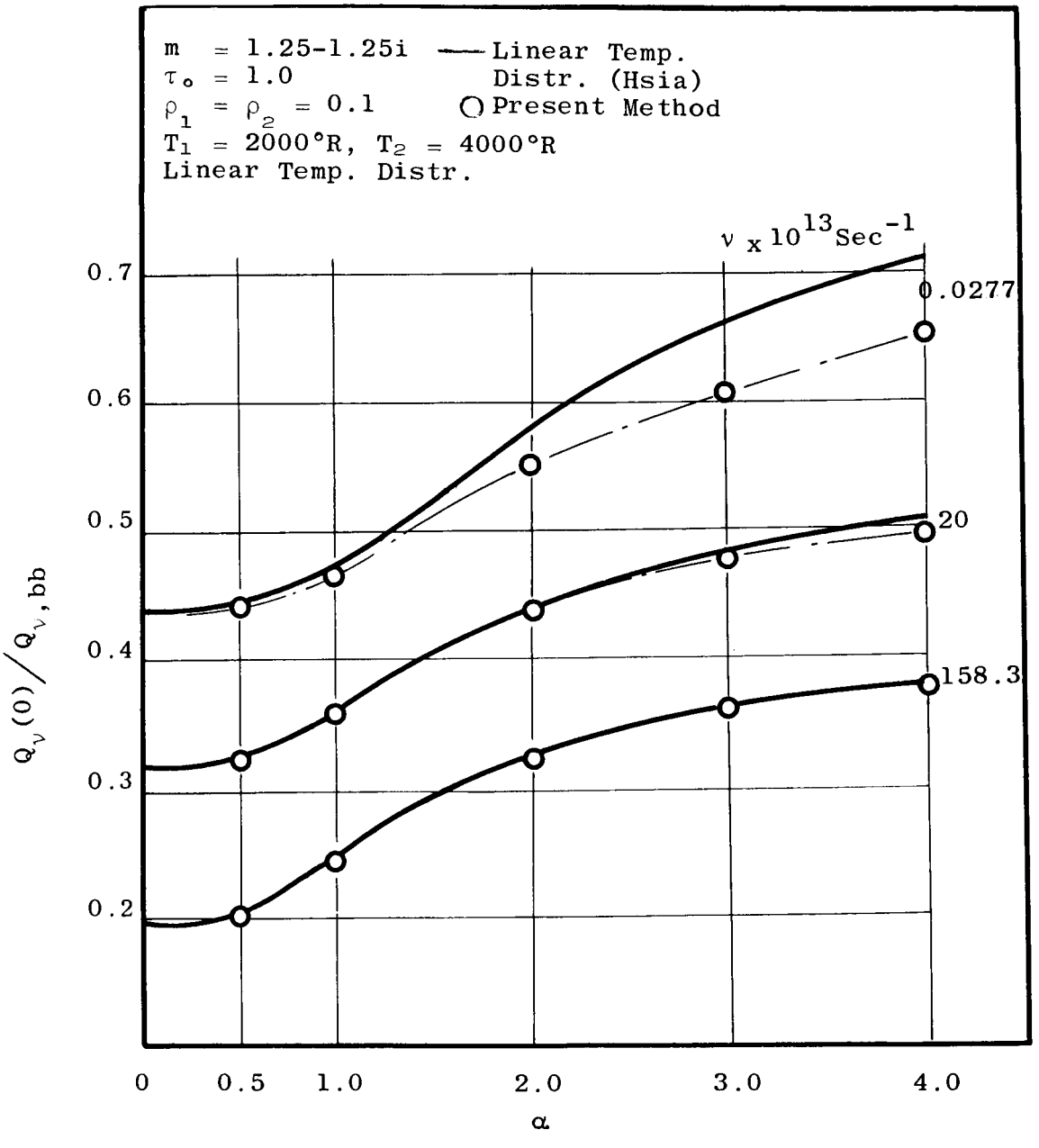

Figure 3. The Effect of Radiative Transfer at Wall 1

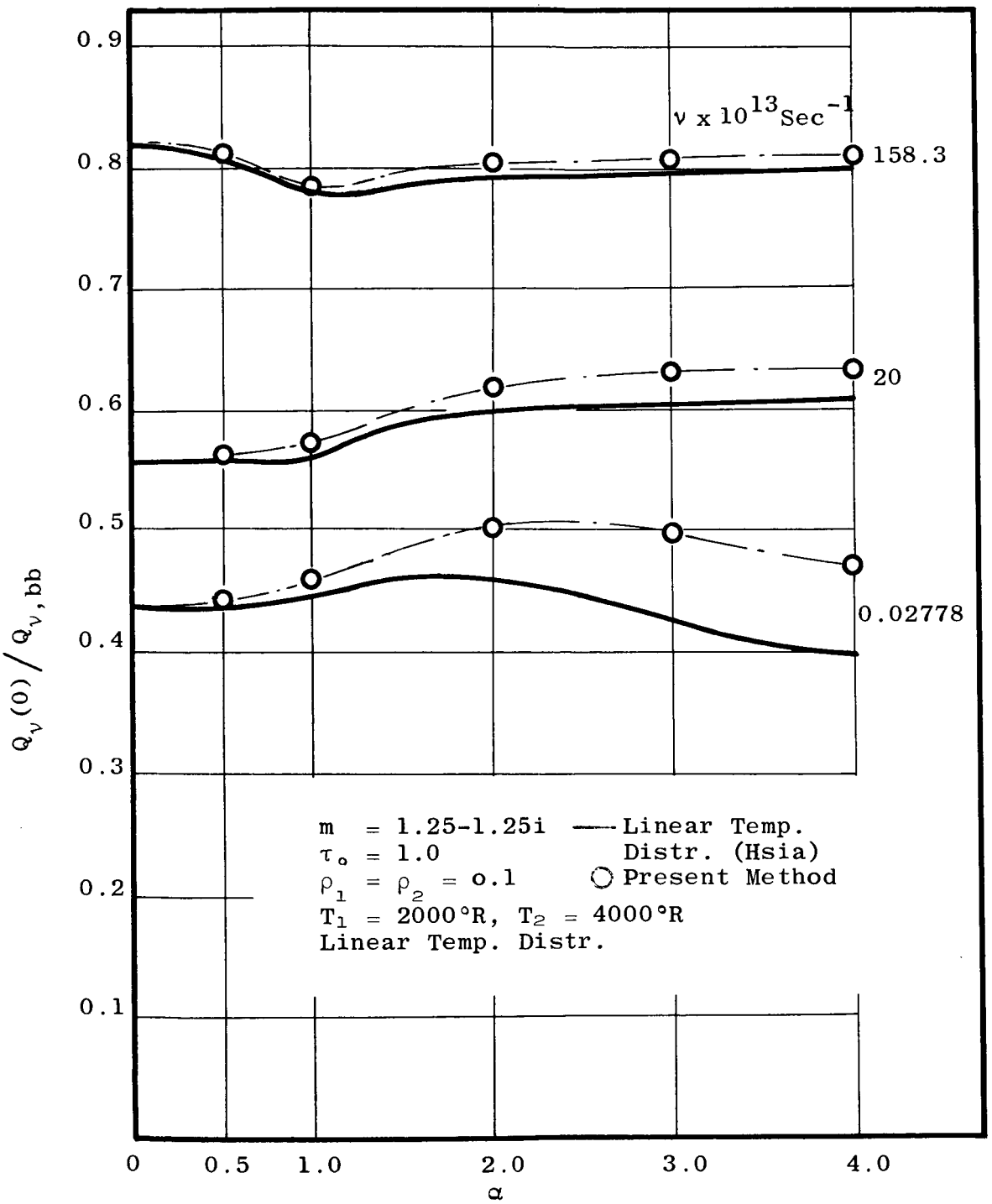

Figure 4. The Effect of Radiative Transfer at Wall 2

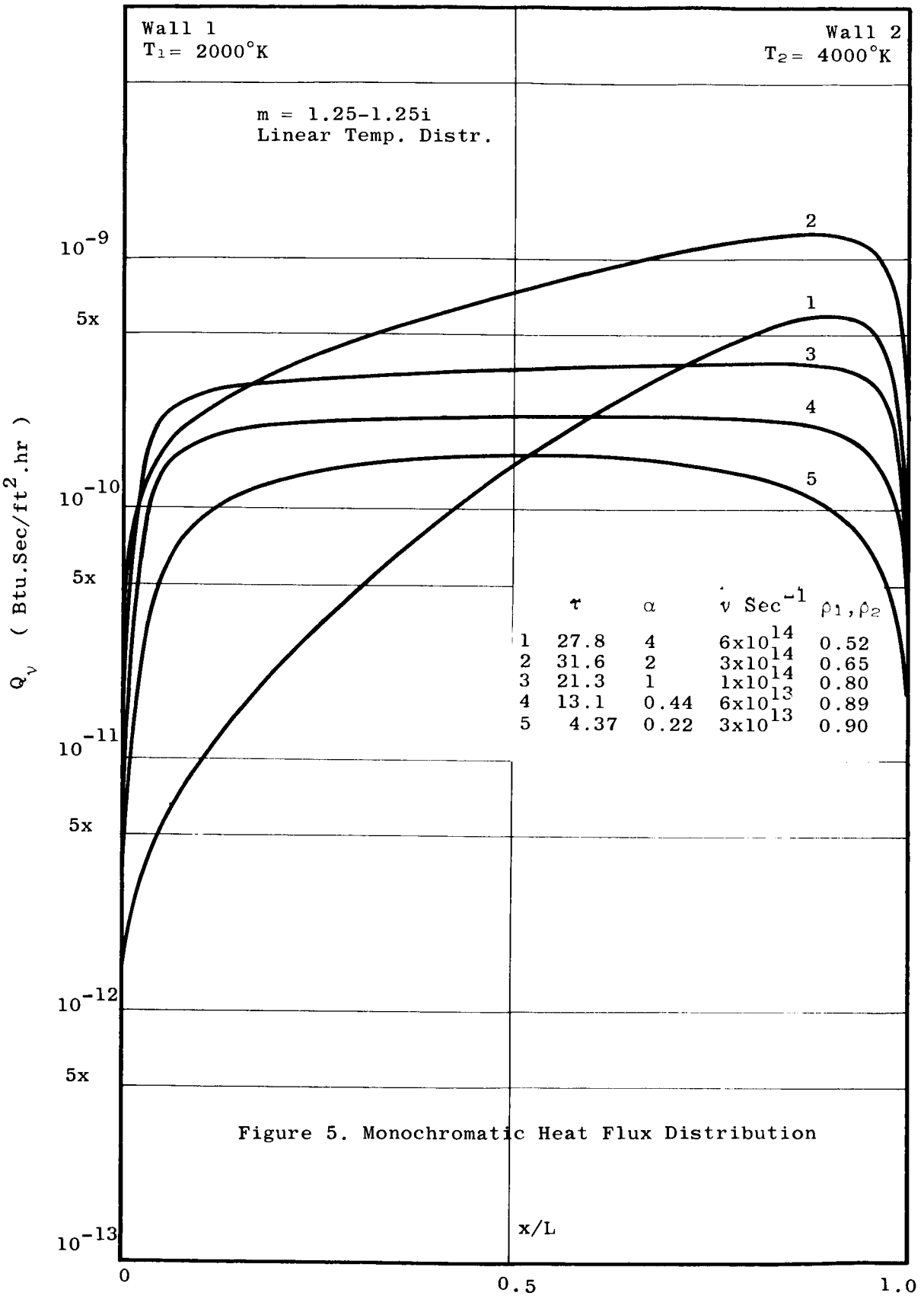

Figure 5. Monochromatic Heat Flux Distribution

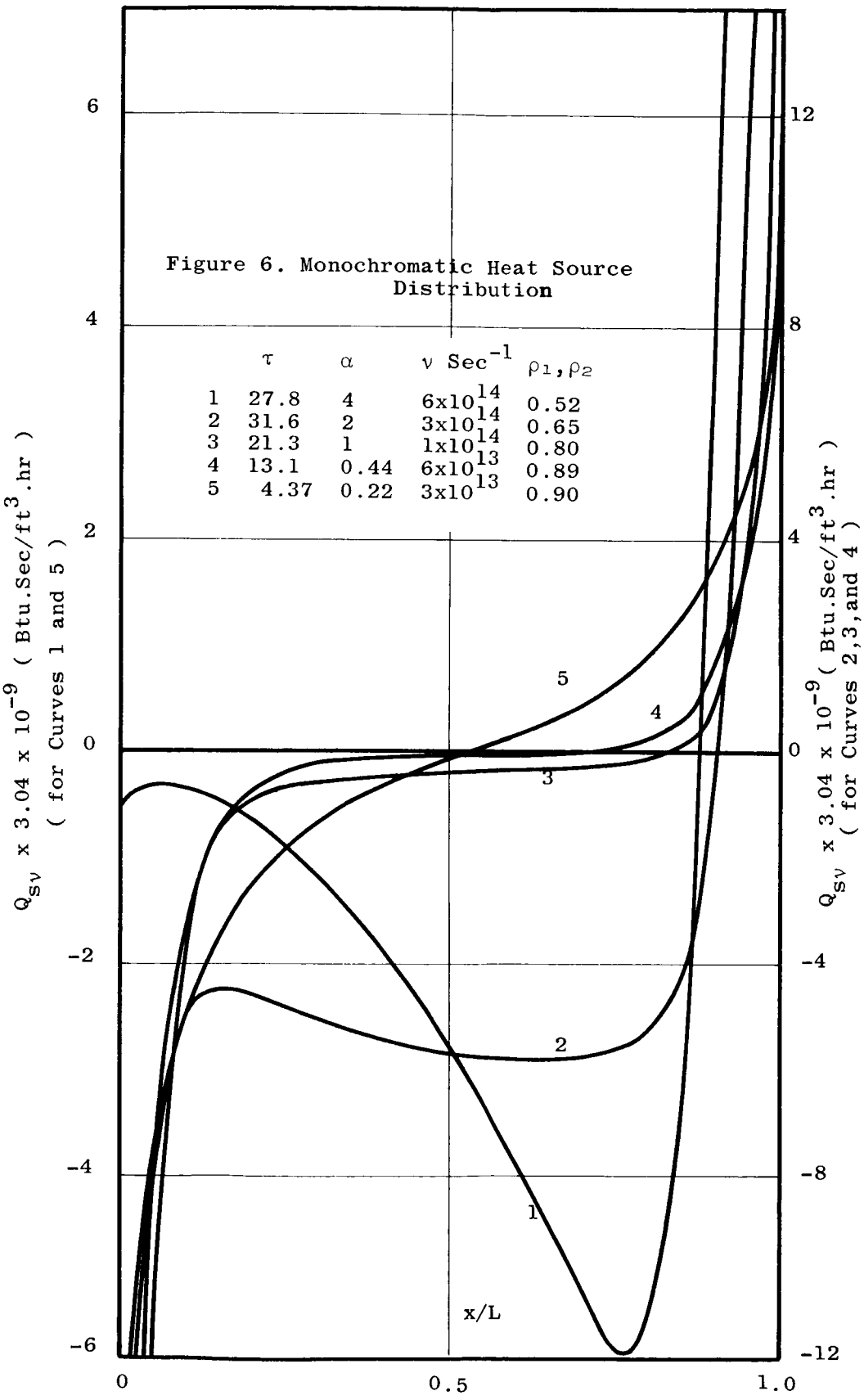
Figure 6. Monochromatic Heat Source Distribution
τ α ν Sec^{-1} ρ1, ρ2
1 27.8 4 6x10^{14} 0.52
2 31.6 2 3x10^{14} 0.65
3 21.3 1 1x10^{14} 0.80
4 13.1 0.44 6x10^{13} 0.89
5 4.37 0.22 3x10^{13} 0.90
Q_{sv} x 3.04 x 10^{-9} (Btu.Sec/ft^3.hr) (for Curves 1 and 5)
Q_{sv} x 3.04 x 10^{-9} (Btu.Sec/ft^3.hr) (for Curves 2,3,and 4)
x/L
6
4
2
0
-2
-4
-6
12
8
4
0
-4
-8
-12
0
0.5
1.0
1
2
3
4
5

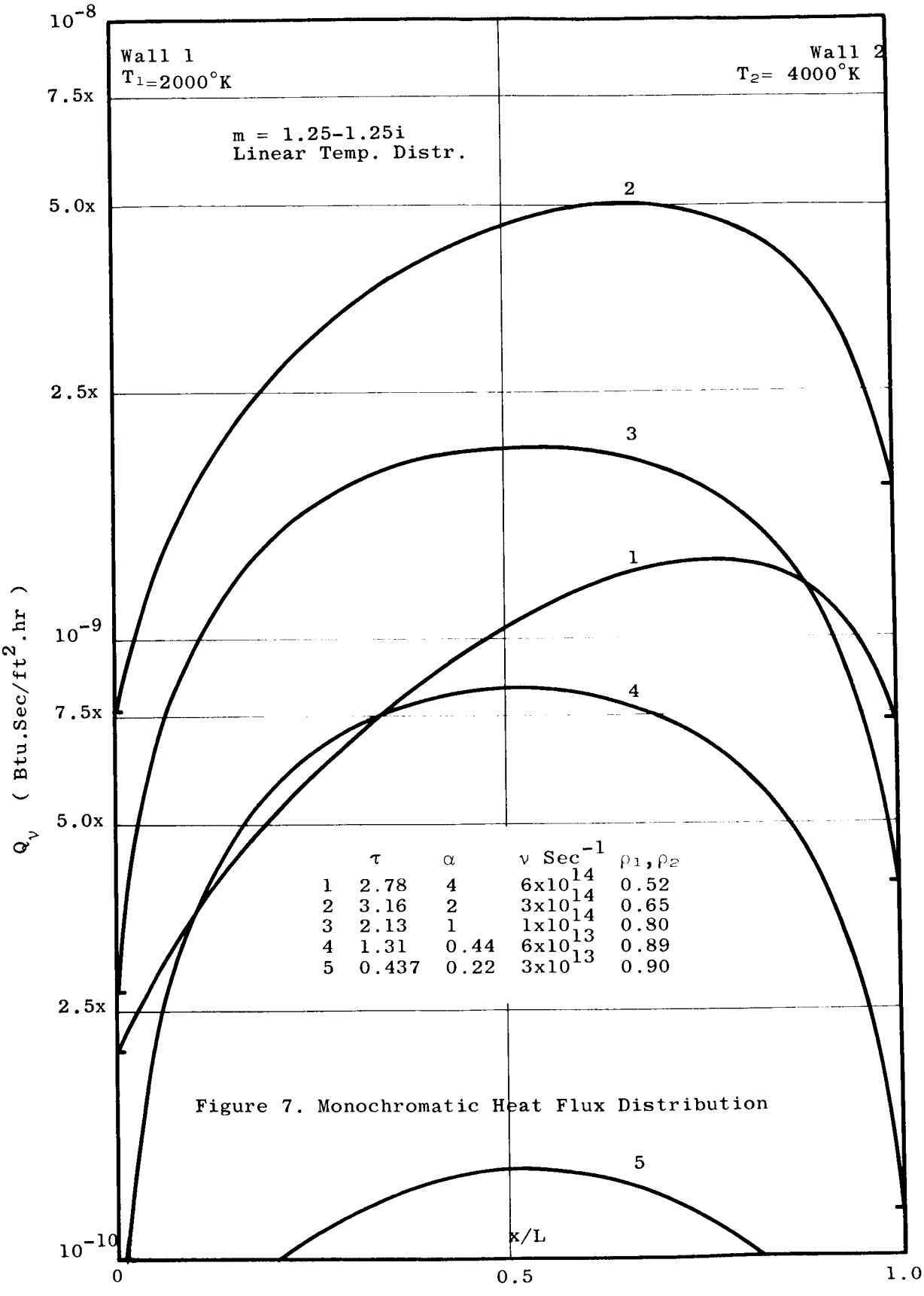

Figure 7. Monochromatic Heat Flux Distribution

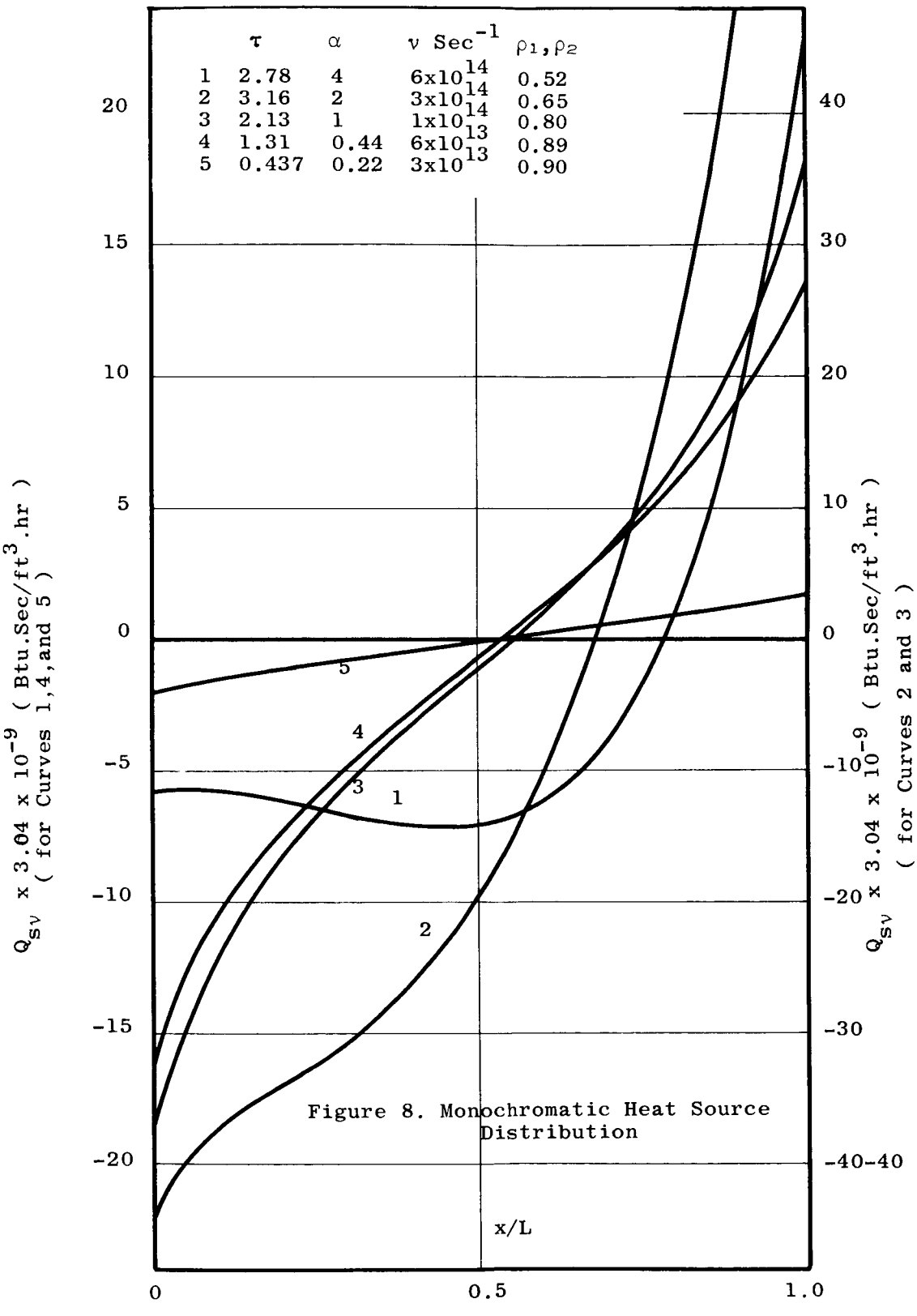

Figure 8. Monochromatic Heat Source Distribution

NASA-Langley, 1968 —— 21 CR-1023